BSPE 00433-686-5

해저지질구조 규명을 위한 지자기 삼성분 자료처리 및 해석기술 연구

A Study on Processing and Interpretation of Three Component Magnetic Data for Subsuface Structure

1994. 5

한 국 해 양 연 구 소

제 출 문

한국해양연구소장 귀하

본 보고서를 "해저지질구조 규명을 위한 지자기 삼성분 자료처리 및 해석기술 연구"과제의 최종보고서로 제출합니다.

1994년 5월

연구책임자 : 박 찬 홍
연 구 원 : 박 건 태
정 백 훈
장 재 경
연 구 조 원 : 주 용

요 약 문

Ⅰ. 제 목

해저지질구조 규명을 위한 지자기 삼성분자료 처리 및 해석기술 연구
(A Study on Processing and Interpretation of Three Component Magnetic Data for Subsuface Structure.)

Ⅱ. 연구개발의 목적 및 중요성

해상에서는 측정원리와 자료처리의 간편성으로 인하여 지자장의 주요 세 방향성분이 합성된 전 자기장을 측정하여 사용하는 것이 가장 일반적이었다. 그러나 전자기장 측정은 방향성분이 없는 자기장의 세기만 알 수 있으므로 자화특성이 복잡한 지질구조를 해석하는 데는 제한적일 수 밖에 없다. 또한 전자기장은 선체자기의 영향을 최소화 하기위해서 감지기를 선체와 최대한 이격시켜 설치해야하므로 취급이나 설치가 불편하다.

그러나 최근 선상삼성분자력계 (STCM: Shipboard Three Component Magnetometer)의 개발과 활용(Isezaki, 1986)으로 해상에서의 지자기 삼성분 측정이 가능하게 되었으며 여러형태의 해석기법의 연구(Seama *et al.*,1990; Nogi *et al.*,1990; Kitahara *et al.*, 1993; Seama *et al.*, 1993)가 뒤이어졌다. 해상 지자기 삼성분자력계는 지하지질에 의한 자기장을 지자기 북향, 동향 및 연직방향으로 분리하여 측정하므로 각 방향 고유의 자기장 진폭을 그대로 나타낼 수 있다. 삼성분 자력이상은 자화복각의 방향, 크기와 자화강도를 산출하는 데 이용할 수 있을 뿐 아니라 전자력이상에 비해 해양지각에 의한 자기선구조를 보다 뚜렷이 보여주기 때문에 해저확장관련 해양지각의 구조와 생성역사등 지질환경 및 구조 해석에도 활용할 수 있다. 특히 단일 측선의 자기

이상 자료로써도 자기이상을 유발하는 자화물체의 자기적 경계, 주향 및 분포 특성(2 차원 또는 3 차원)을 파악할 수 있기 때문에 기존의 전자기이상에 비해 지질구조 해석의 보다 강력한 도구가 될 수 있다.

육상의 측정에 비해 상당히 많은 기술적 문제를 포함하는 해상삼성분자력의 측정과 분석 기술은 최근에 이르러서야 정립되었으며 일본의 치바대학, 동경대학, 고베대학등 일본연구계를 중심으로 활발한 연구가 진행되고 있으나 점차 영역이 확대되가고 있는 추세에 있다. 선체내에서의 자력측정은 실제 지질로부터의 성분외 에도 선체 자체의 자기영향에 크게 지배를 받기 때문에 그들을 분리하는 것이 필요하나 그것은 상당한 기술적 뒷받침이 요구되며 종합조사선 온누리호에 국내 최초로 삼성분 자력계가 설치되고 1994년 이후 활용될 예정인 바 시스템의 원활한 운영과 측정 자료의 처리 및 해석 기술의 토대 마련을 위한 기반 연구로써 본 연구는 중요성을 갖는다. 또한 삼성분자력자료는 해양지각의 구조 및 생성연대 등의 연구에 매우 효과적으로 활용될 수 있기 때문에 동해지역의 해양지각의 성인과 관련한 연구 및 심해저 광물자원탐사를 위한 지질환경 연구 기반을 다지는 데에도 중요한 목적이 있다.

Ⅲ. 연구내용 및 범위

해상 삼성분 자력계의 측정원리, 선체자기보정과 자화구조 파악에 매우 효과적인 2 차원 자화층 해석등에 필요한 이론적 배경의 검토 및 자료 처리 기술을 확립하고 동해 울릉분지상에서 획득된 실자료를 처리, 검증하였으며 그 결과를 중심으로 울릉분지의 지질구조를 해석하였다.

Ⅳ. 연구결과 및 활용에 대한 건의

삼성분 자력계의 원리 및 운영기술이 파악됨으로써 온누리호 삼성분자력계의 활용의 토대를 마련함과 아울러 선체자기의 보정방법 및 산출된

vector 자기이상을 이용한 지질구조 해석 기술을 제시하였다. 본 연구결과를 요약하면 다음과 같다.

(1). 삼성분자료처리 소프트웨어를 연구소시스템에 적합화함으로써 활용 가능하도록 하였다.

(2). 조사지역 3 개 지점에서 특별히 실시된 "8" 자 형태의 선회측정 자료로부터 이어도호의 선체자기 계수가 산출되었다.

(3). Gyro, roll, pitch등 선체의 운동상태는 측정되는 세 방향 자기성분에 매우 큰 상관성을 가지고 변화하였으며, 그 영향은 보정처리에서 대부분 제거되었다. 그러나 gyro자체의 측정정밀도의 불량으로 동측성분(Y-component)에 상당한 오차가 잔류되고 있음이 관측 되었으며 이는 선체 운동에 대한 정밀도 높은 측정이 필요하다는 것을 제시한다.

(4). 선체자기와 IGRF 보정된 자력치로부터 proton 자료에 대한 STCM의 측정오차를 이용한 noise filter의 결정과 적용으로 삼성분 자기이상을 산출하였다.

(5). 공간미분기법을 이용하여 자화층의 경계 및 주향을 산출한 결과 2-3 개의 주요 자화층의 방향성이 파악되었으나 gyro 측정오차로부터 기인한 동측성분의 지나친 진폭으로 북쪽 편향성을 나타냈다.

(6). 연직성분은 북향성분에 비해 진폭이 크게 나타나는 것은 이 지역 자기장의 복각이 비교적 크다는 것을 지시한다.

(7). 울릉분지내 연직성분(Z-component)는 분지내 기반암의 윤곽을 표현한다. 즉 기반암이 낮은 분지 북서부와 남부 및 서부의 분지주변에서 고이상대가 중앙에서 음이상대가 주로 분포하며 분지내 고이상대들은 관입암체등에 의한 기반암의 돌출에 의한 것으로 해석된다. 분지중앙의 저이상대는 두꺼운 퇴적층과 맨틀의 천부 존재에 기인한다.

(8). 삼성분 자기이상은 proton 자기이상에 비해 보다 뚜렷한 남서-북동 방향성을 나타내며 분지 지질구조의 발달 방향을 지시한다.

(9). 북향,동향 자기이상분포의 북서부에서 남서-북동방향성의 자기

이상대가 나타나고 있으나 분지내에서 해저확장과 관련된 선구조는 파악하기 어렵다.

(10). 삼성분자기이상은 전자력이상에 비해 보다 많은 지질구조에 대한 정보를 표현하기 때문에 기존의 전자력 이상에 의한 것에 비해 보다 구체적이고 정확한 지질구조를 파악할 수 있으므로 현재까지 여러 가지 연구방법의 적용에도 불구하고 그 성인 및 발달 역사가 불명확하여 논란중인 동해분지 연구, 대륙붕자원 탐사를 위한 지질 환경 연구 및 심해저 광물자원탐사 지역인 태평양 지역등의 해저지각구조나 확장역사등의 연구에 중요한 결과를 제공할 것으로 기대된다.

CONTENTS

List of Tables

List of Figures

Introduction

Vector data of the geomagnetic field can provide us with much more direct and clear information than total intensity in interpreting subsurface structure irrespective of its dimensionality. Such a demand has been accomplished with development and successful operation of the STCM(Shipboard Three Component Magnetometer; Isezaki *et al.*,1981; Isezaki, 1986). The STCM has been used as a strong tool to interprete seafloor tectonics in several authors(Kitahara *et al.*,1984; Seama *et al.*, 1990; Seama and Isezaki, 1990; Nogi *et al.*, 1990; Kitahara *et al.*,1993; Seama *et al.*, 1993) due to its particular advantages.

Because the vector anomalies are shown up in a high amplitude with reference to specified direction whereas total intensity anomaly are often distorted on account of an orientation of the ambient field and magnetic lineations, more obvious correlation with magnetic structure can be easily understandable. Recently very effective method was presented to provide the positions and strikes of magnetic boundaries in two dimensions or three dimensions using spartial differential vectors(Seama *et al.*,1993). The method allows us reasonable tectonic interpretations through an identification of magnetic lineations related to the seafloor spreading, pseudo-faults, fracture zones and central anomaly.

The measurement with the STCM fixed on the ship is generally accopanied by magnetic interferences arisen from several magnetic sources as well as the ship itself. However it is still hard to completely isolate those noises due to accuracy problems of the ship's tilting angles rather than the processing method itself. The noises remain behind calculated anomalies even after the ship's magnetic effect is theoretically removed using twelve ship's matrix constants(Isezaki, 1986). Such noises can be secondarily removed using a moving average technique or a optimal filter constructed from power spectra of proton anomaly and noise which is defined as difference between a proton

anomaly and the STCM anomaly.

In present research the optimal filter method proposed by Korenaga(1994) will be applied to obtain theoretically noise free geomagnetic field vectors. And then the anomalies will be used to determine the position and strike of magnetic structure by applying spartial defferential method and interpreted geologically. Since deep seismic or direct drilling data are little available in the Ulleung Basin(the Tsushima Basin) where dating and mechanism of its formation is still the point at issue, application of three component anomaly may bring out a clue to explain it if it was formed by seafloor spreading as postulated in previous reseaches(Otofuji and Matsuda, 1987; Chough and Lee, 1992; Yoon and Chough, 1992; Suh, Lee, and Suk, 1993).

This study presents a preliminary result on analysis and brief interpretation in geology of three component magnetic vector data which were obtained by the joint cruise of Korea and Japan in the Ulleung Basin(Fig.1).

Ship's Magntic Constants and Geomagnetic Vector Fields

Since the STCM measures the magnetic field with fixed on board, it could include the ship's remanent and induced magnetic fields as well as the ambient magnetic fields which will be finally derived. Isezaki(1986) presented how the ship's magnetic effect can be isolated from the measurements.

The measurement by the STCM can be expressed as

$$\mathbf{H}_{ob} = \mathbf{F} + \mathbf{H}_i + \mathbf{H}_p \qquad (1)$$

where $\mathbf{H}_{ob}$, $\mathbf{F}$ are the observed and the ambient field, and $\mathbf{H}_i$, $\mathbf{H}_p$ are the ship's permanent and induced magnetic fields, respectively.

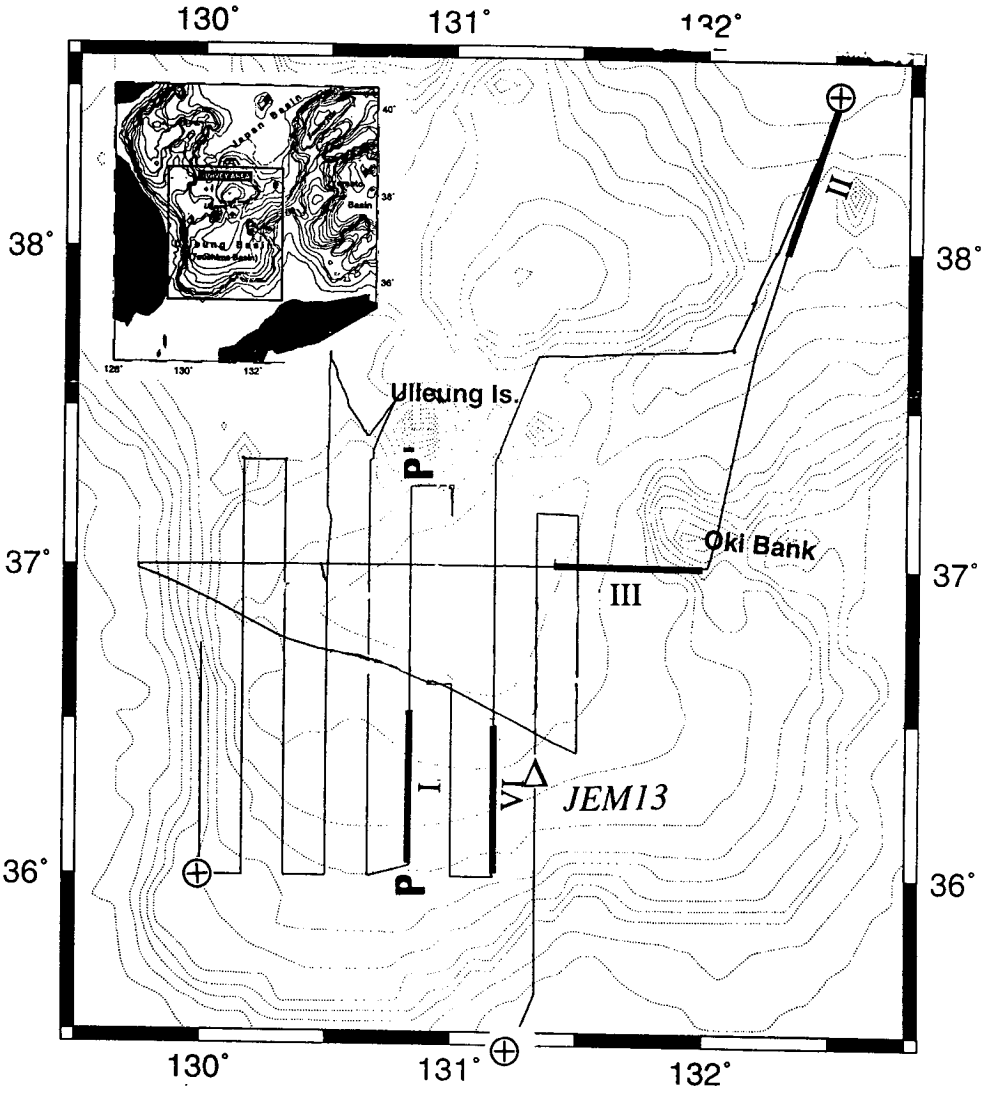

Fig.1. Survey location and tracks of the STCM and gradiometer in the Ulleung Basin. Location of the OBEM observation is denoted as a triangle mark(*JEM13*). Circles with cross mark are locations where the "8" shaped rotation was operated. Inset shows the survey location. Dashed contours represent bathymetry based on ETOPO in an interval of a hundred meter.

The magnetic fields induced at the ship, $\mathbf{H}_i$, linearly depend on **F**, that is,

$$\mathbf{H}_i = \mathbf{AF} \qquad (2)$$

where **A** is a 3x3 matrix related to magnetic susceptibility of the ship's body, location of the sensors, and shape of the ship. Because the three fluxgate sensors are rigidly fixed to the ship with orthogonal axes each other so that each could be oriented toward the bow and the starboard, and downward, respectively, **F** needs to be transformed by coordinate rotation with regard to roll, pitch, and yaw of the ship. The equation (1) will be rewritten by considering the ship's movement as

$$\mathbf{H}_{ob}=(1+\mathbf{A})(\mathbf{RPY})\mathbf{F} + \mathbf{H}_p \qquad (3)$$

where **R**,**P**,and **P** are the matrices of the coordinate rotation as for the roll, pitch, and yaw of the ship, respectively.

Therefore the geomagnetic field, **F**, can finally be obtained from the following equation

$$\mathbf{F} = [(1+\mathbf{A})\mathbf{RPY}]^{-1}(\mathbf{H}_{ob}-\mathbf{H}_p) \qquad (4)$$

Because **A** and $\mathbf{H}_p$ are constant, the geomagnetic field **F** can be estimated from the observeed $\mathbf{H}_{ob}$, **R**,**P** and **Y** if **A** and $\mathbf{H}_p$ are determined. The constants **A** and $\mathbf{H}_p$ are calculated from sets of omnidirectional rotation data at locations where **F** are known(if **F** is not available, the IGRF will be sufficient).

Optimal Filter for Noise Isolation

Measurement of magnetic fields using the STCM contains number of noises as well as geomagnetic field as a signal because the STCM is usually attactched to the ship's body for the measurement. The measurement errors of the STCM can be defined as the difference between total intensity anomaly from the STCM and one from the proton precession magnetometer as a signal because the total intensity by the proton precession magnetometer is generally noise free compared to one of the STCM.

An optimal filter can be constructed by carefully treating with the measurement error of the STCM as stated in the above compared with a proton precession magnetometer data in frequency domain. Korenaga(1994) presented how to isolate the noises using the optimal filter(Wiener filtering) from ratio of the power spectra of signal and noise to enhance a quality of the STCM data.

The optimal filter can be defined in the wave number domain as (Press *et al.*, 1992)

$$\Phi(f)=\frac{|\mathbf{S}(f)^2|}{|\mathbf{S}(f)^2|+|\mathbf{N}(f)^2|} \qquad (5)$$

where $\Phi(f)$, $\mathrm{S}(f)$ and $\mathbf{N}(f)$ represent the optimal filter, the power spectrum of the signal, and the noise in the wave number domain.

More reliable optimal filter can be constructed by estimating power spectrum from as many sampled proilfes as possible, because the standard deviation can be reduced at a rate of $1/\sqrt{N}$ for N profiles long enough not to suppress any long period of anomalies.

The Position and Strike of Magnetic Boundary

Three component field vectors can be effectively used to determine a

position and strike of boundary of the magnetic structure in two dimension. Seama *et al.*(1993) proposed a method to satisfy such a purpose using a concept of the spatial differential vectors. Peak of spatial differential vectors from three component anomalies is located at the boundary of magnetic structure and the strike of the magnetic boundary can be determined from a concept that the magnetic field is expected to be zero along the boundary.

The intensity of spartial differential vectors(ISDV) on a magnetic structure as drawn in Fig. 2 is defined as:

$$\left|\frac{\partial F}{\partial y}\right| = \sqrt{\left(\frac{\partial F_x}{\partial y}\right)^2 + \left(\frac{\partial F_x}{\partial y}\right)^2 + \left(\frac{\partial F_x}{\partial y}\right)^2} \qquad (6)$$

According to the above equation the ISDV will be maximum at a magnetic boundary where y=0. Subsequently the boundary of the magnetic structure can be traced independent of the magnetization of the magnetic structure(Fig. 3). If magnetic profile lies obliquely to strike of the boundary at an angle α from the X-axis, then the ISDV can be estimated by substituting $\left|\frac{\partial F}{\partial y}\right|$ of the equation (6) for $\left|\frac{\partial F}{\partial y}\right| \times \sin \alpha$ except for a profile parallel to the X axis.

Therefore for the fixed earth's coordinate system, the ISDV can be given by

$$\left|\frac{\partial F}{\partial p}\right| = \sqrt{\left(\frac{\partial F_n}{\partial p}\right)^2 + \left(\frac{\partial F_e}{\partial p}\right)^2 + \left(\frac{\partial F_d}{\partial p}\right)^2} \qquad (7)$$

where F_n, F_e, F_d are the northward, eastward and downward components of the geomagnetic anomaly field, respectively.

Since component of the magnetic anomaly parallel to the boundary vector is zero,

$$\mathbf{F} \cdot \mathbf{U} = 0. \qquad (8)$$

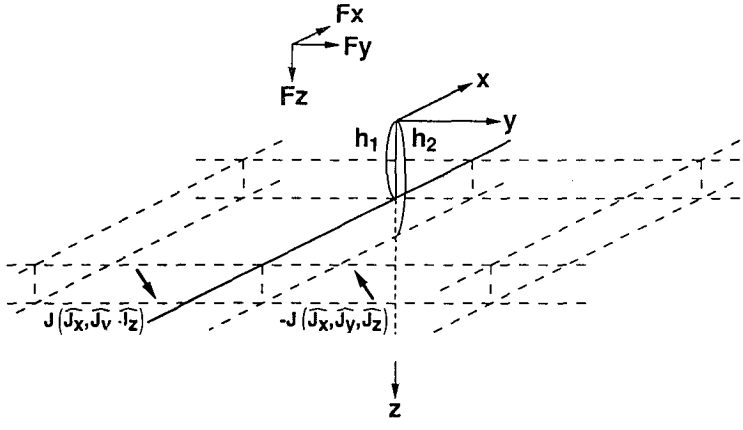

Fig.2. Geometry for deriving the magnetic field vector caused by a two-dimensional magnetic structure(Seama *et al.*,1993)

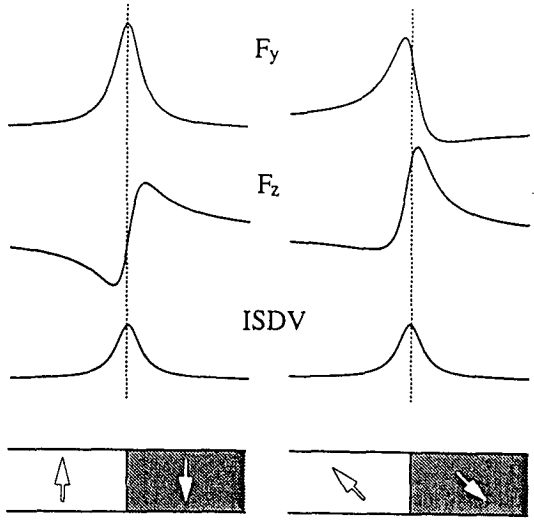

Fig.3. The ISDV calculated from magnetic field components of two dimensional magnetic structure. The peaks in the ISDV profiles are always located just at the magnetic boundary independent of magnetization of the structure.

is valid on the magnetic boundary , where U is defined as a unit vector parallel to the boundary. Considering some bias F_b in measurement and from IGRF removal, the equation (8) can be rewritten as

$$(\mathbf{F} - \mathbf{F}_b) \cdot \mathbf{U} = 0. \qquad (9)$$

Three components of unit vector U and constant term $\mathbf{F}_b \cdot \mathbf{U}$ can be estimated using the least-square operation. The validityof the equation (9) implies that the boundary vector U can be determined irrespective of any biases existed in geomagnetic anomalies because all the biases are confined in the constant term. The strike of the magnetic boundary can be given using the northward and eastward components of unit vector, U_n and U_e.

Acquisition

The STCM of the Chiba University was installed on board of the R/V Eardo belonged to KORDI(Korea Ocean Research and Development Institute) and run for the whole survey period. The STCM is composed of a vector flux-gate magnetometer, a proton precession magnetometer, a gyrocompass, a vertical gyroscope, and a microcomputer(Fig.4). The flux-gate sensor with three orthogonal axese was set on top deck of the ship to avoid noises from mixing with signals as far as possible.

In laboratory were installed a console and a microcomputer to control the STCM, to log and to display input signals in real time. A three dimensional gyro was also at the same time operated to observe heading, rolling, and pitching angles of the ship. The signals from the flux-gate sensors and the gyro are finally recorded in every one second into the microcomputer through averaging after primarily storing in a sampling rate of 0.1 sec in the controller. Fig.5 shows example profiles of the magnetic fields measured from three axes of a

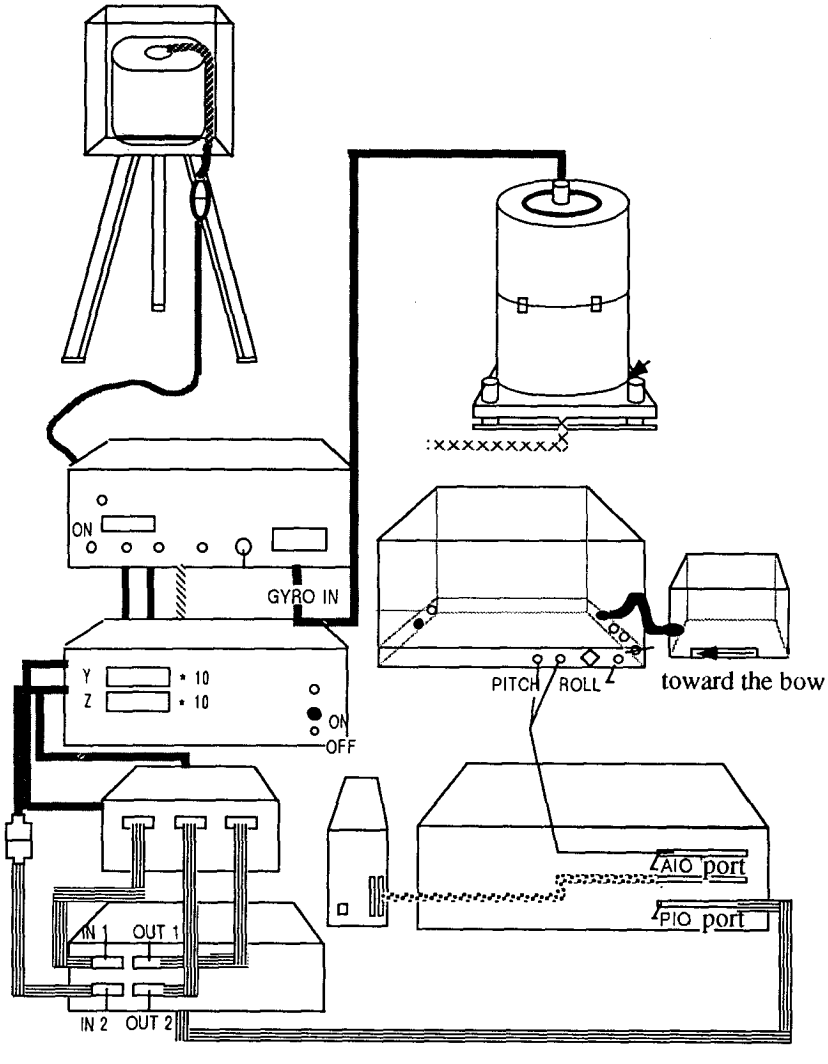

Fig.4. Schematic diagram of three component measurement by the STCM(Shipboard Three Component System) used in this survey.

fluxgate sensor and heading, rolling and pitching data.The ship's positions were gathered using a GPS system of the R/V Eardo and monitored for ship's steering along the planned survey lines. Data of positioning and water depth were simultaneously logged into a microcomputer in one second interval.

The magnetic observations were specially made along two circled tracks with an opposite direction at four locations(Table 1) to determine the ship's magnetic field.

Table 1. Date and positions of the "8" shaped operation.

Date	Latitude	Logitude
Aug. 31, 1992	37°20.34'	129°58.30
Sep. 1 , 1992	35°59.54'	130°0.12
Sep. 5 , 1992	38°26.93'	132°30.51
Sep. 7 , 1992	35°29.50	131°15.64

Data Processing

Since the STCM measures magnetic field with being fixed on board, not only magnetic fields generated from the ship's body but also the ambient geomagnetic field would be inevitably mixed up together. Generally the magnetic field originated from the ship fairly varies with the motion together with magnetic properties of the ship's body as well expressed by the equation (4). Data processing should be as a first step devoted to seperation of the ship's magnetic effect from the observed magnetic data.

Twelve constants in the ship's magnetization matrix were estimated using three component data measured during the "8" shaped cruises at three different

locations. A set of "8" shaped rotation data observed in the beginning stage among four sets was excluded in estimating twelve constants because the gyro sensor was somewhat shifted. The ship's magnetization constants derived are shown as in Table 1.

The constants determined were applied to the equation (4) to obtain the geomagnetic field vectors by seperating the ship's induced and permanent from the magnetic field measured on board. The IGRF and a linear trend were removed to derive residual magnetic field vector of each component and total intensity anomaly. Fig.6 shows three component magnetic anomaly and total intensity anomaly profiles in the earth's coordinate after the ship's magentic, the IGRF90, and a linear trend are eliminated from the observed magnetic profiles of Fig.5.

Table 2. Twelve constants of the ship's magnetization determined from the "8" shaped rotations of three locations.

$$A = \begin{vmatrix} 1.10906 & 0.09778 & 0.06456 \\ -0.16929 & 1.17888 & 0.06093 \\ 0.04158 & 0.07634 & 0.92181 \end{vmatrix}$$

$$H_p = \begin{vmatrix} 12121.3 \\ 5355.6 \\ 9721.9 \end{vmatrix}$$

The short wave length anomalies probably classified as noises were filtered using a optimal filter constructed from the ratio as defined in the previous equation (5). Power spectra for each anomaly of the STCM and proton were at first estimated and then ratio was calculated from power spctra of singals and noises for several magnetic profiles long enough not to suffer a

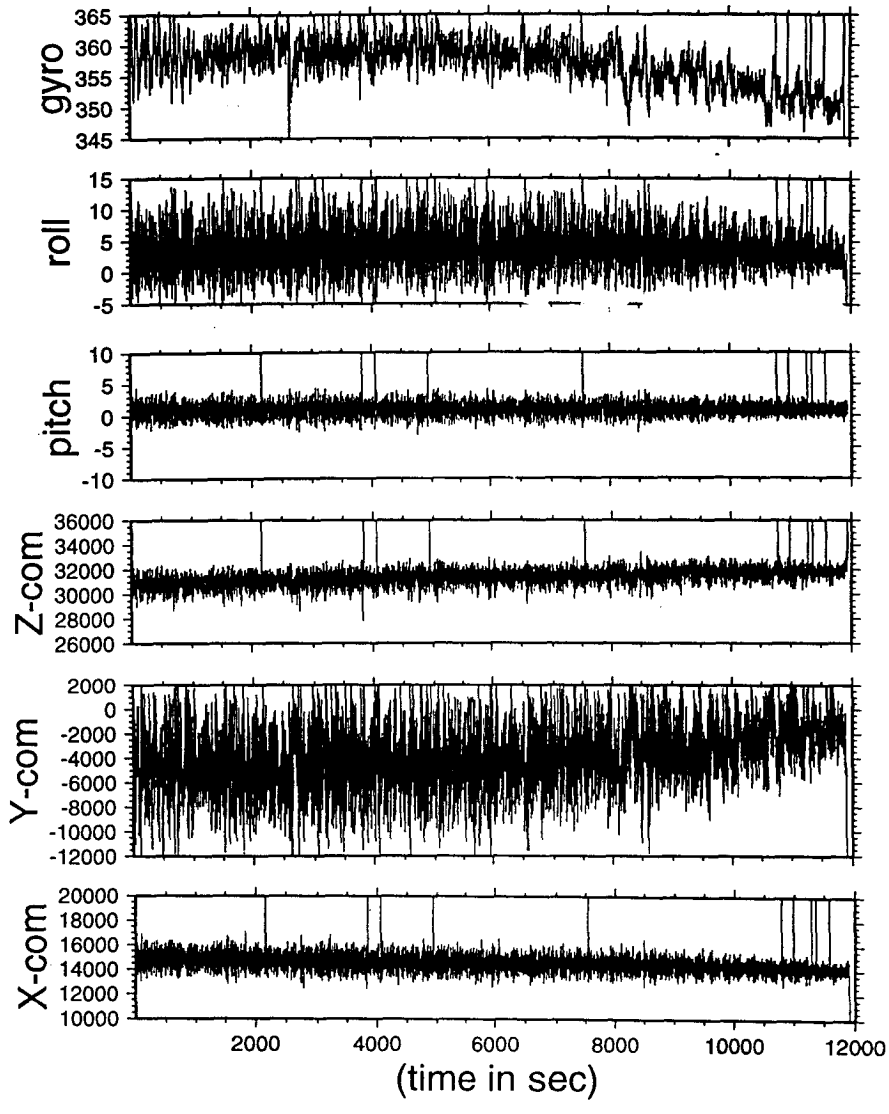

Fig.5. An Example of observation profiles for three component magnetic fields in ship's coordinate by the STCM and heading, roll, and pitch by the Chiba University's gyrocompass and verical gyroscope in this survey.

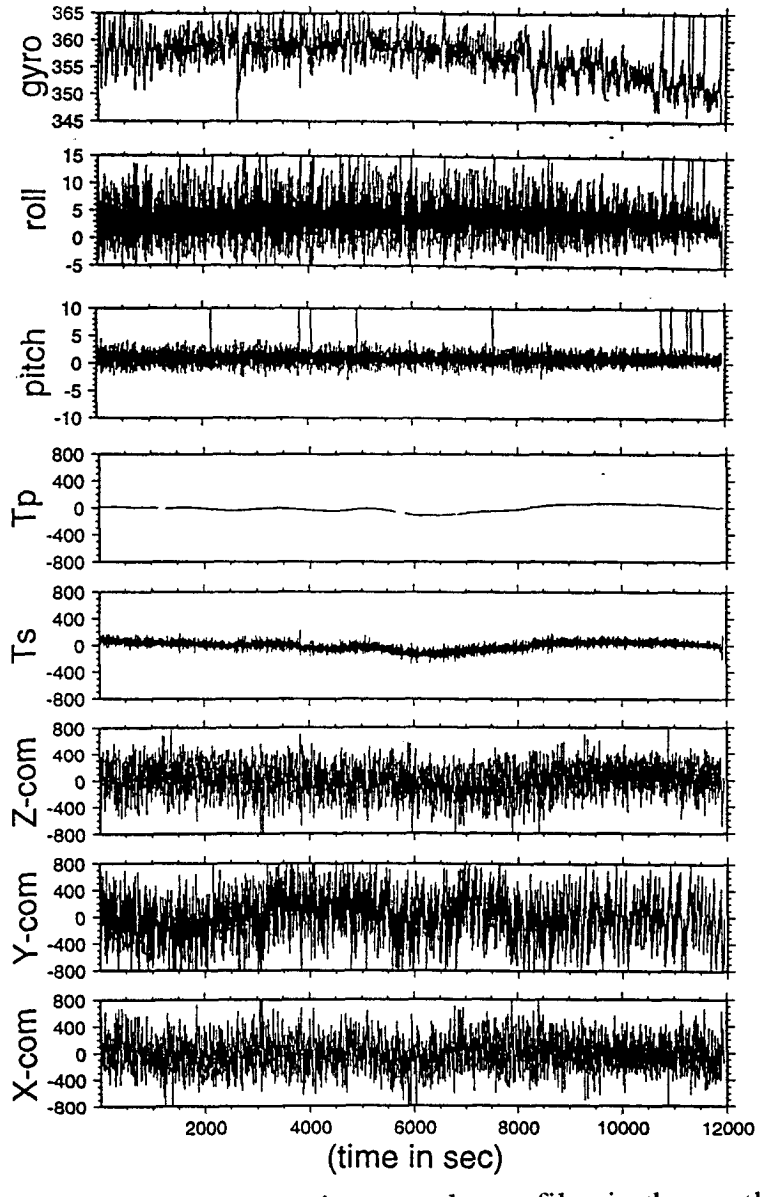

Fig.6. Three component magnetic anomaly profiles in the earth's coordinates after the ship's magnetic fields are isolated from the observations of Fig.2 and comparison of total intensity anomaly from the STCM and from a proton precession magnetometer. T_p and T_s are total intensity anomaly from a proton precession magnetometer and one calculated from three components of the STCM, respectively.

loss of anomaly with a typical wavelength in the survey area . Where the signal means the total intensity anomaly from a proton precession magnetometer and the noises the differences between anomaly of the STCM and one of the proton magnetometer. Since the noise as well as the STCM anomaly may be linearly biased, such a trend was at first removed before the FFT was applied.

Fig.7 shows the power spectra of signal and noise, and the ratio for four typical magnetic profiles in the survey area. The power spectra of the signals and noises appear as similar features over most of profiles. Power spectra of the signals have a break possibly seperating the signal from the noise around 10 km wavelength and are rapidly suppressed in shorter wavelength region than approximately 10 km, whereas ones of the noises show a strong amplitude even in the wave length shorter than 10 km and a peak amplitude specially around 0.1 km in wave length. The ratios, however, are fairly different from distributions of power spectra in which the noises are cut off. The noises are cut off at approximately 17 km in wave length for a group of profiles(Fig.7-I,II), while another group at around 3.5 km(Fig.7-III,IV). In case which such ratios of the power spectra are stacked and averaged all together regardless of different cut off wavelength to construct a optimal filter, much noises might be not cleared in the profiles which contain the noises longer than cut off wavelength. Accordingly judging from such phenomena a optimal filter is recommened to construct and apply from profile by profile or group by group which retain a similar noise charateristics if possible.

In this study was selected a ratio profile in which the signals and noises are rather clear separated and has a longer cut off wavelength to isolate most of noises as far as possible among several ratio profiles. The selected ratio profile and determined filter are shown as in Fig.8. The filter determined was applied to all the three component and total anomaly profiles. Filtred profiles are shown in Fig. 9.

The east component still appears to be some extent unstable because the noises are originated from accuracy of the gyro from the very beginning of the measurement. The position and strike of magnetic boundaries were determined from three component vector anomalies and presented on magnetic boundary

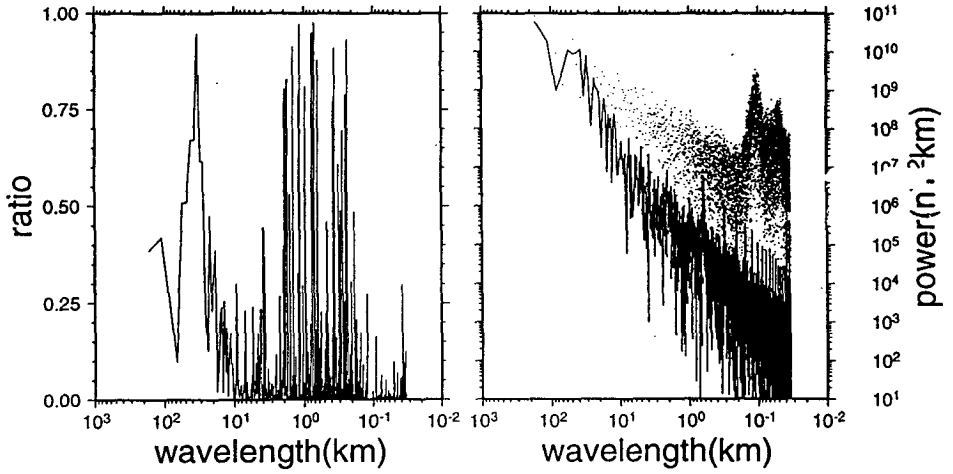

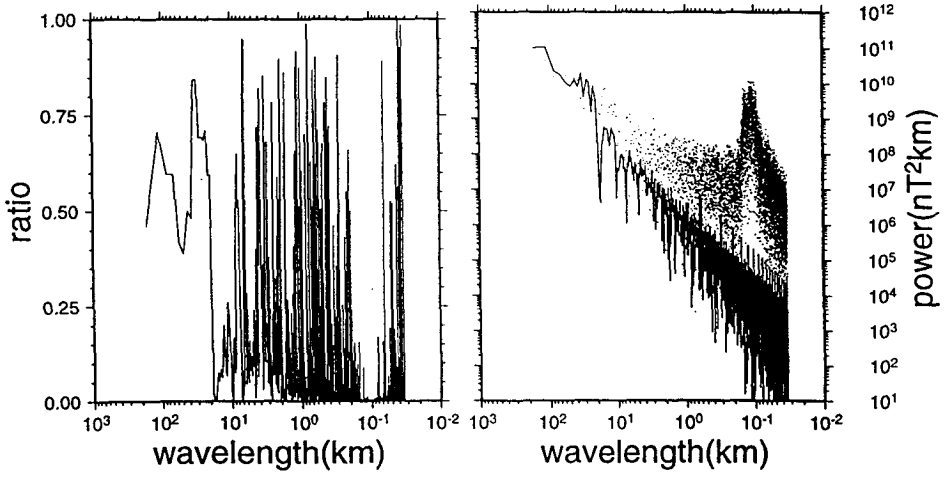

Fig.7. Signal and noise power spectra(right), and ratio($\Phi(f)$)(left) for four typical magnetic profiles I,II,III, and IV as denoted in the survey track map.

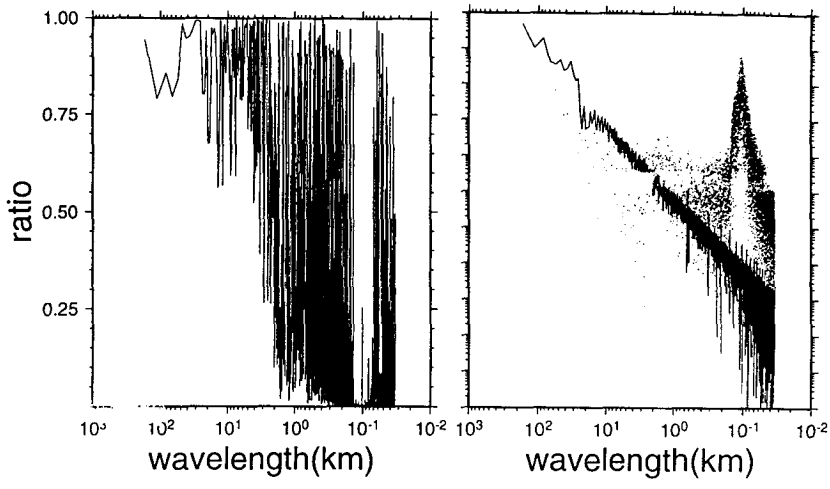

(III)

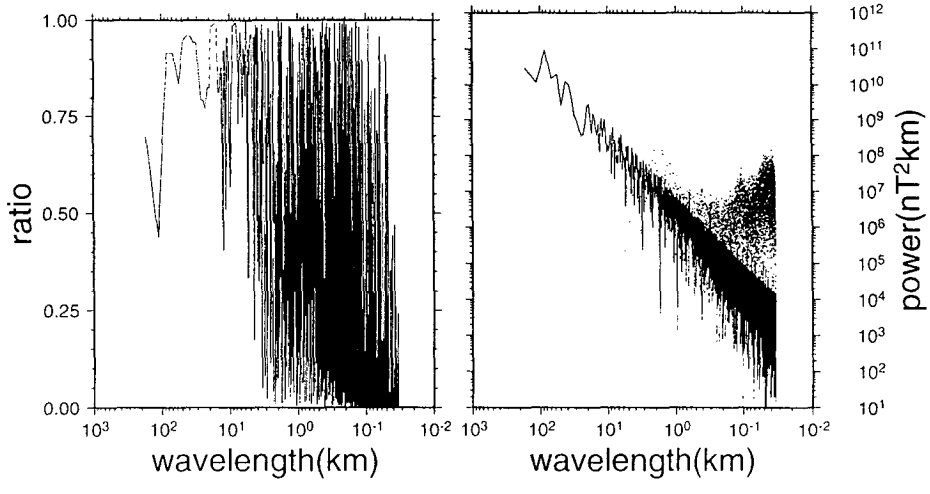

(IV)

Fig. 7. (Continued)

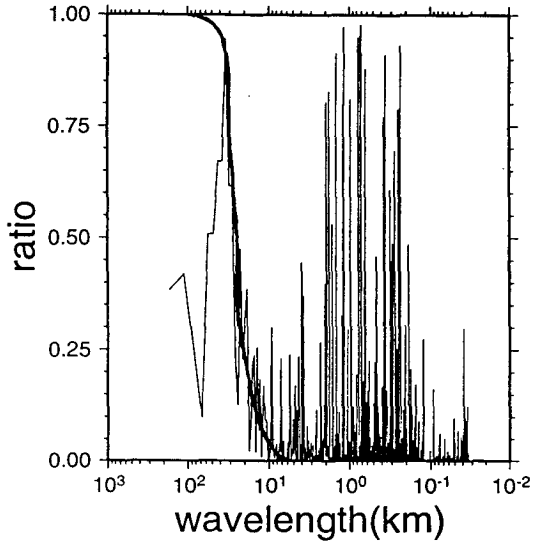

Fig.8. Ratio($\Phi(f)$) and optimal filter applied to remove high wave number noises.

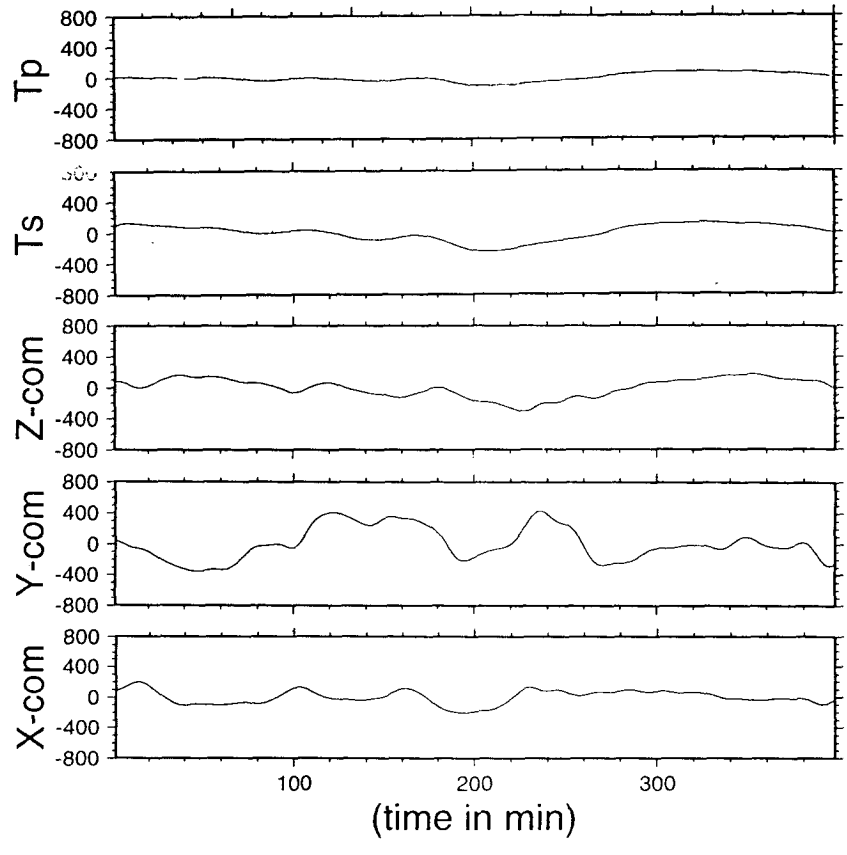

Fig.9. Three components and total anomaly profiles after filtered. T_p and T_s are total intensity anomaly from a proton precession magnetometer and the STCM,respectively.

and strike map.

Result and Discussion

Fig.5 shows the three component magnetic fields of X, Y, Z for the ship's coordinate, the bow, the starboard and downward, respectively and heading, rolling, and pitching along a S-N trending profile. The ship's heading and rollling are severely fluctuating with various periods and a large change whereas the pitch is rather stable. Especially in general trend the starboard component drastiaclly varies in accord with the heading change. Unstable measurement of the ship's tilt angles appears in most of observed data, which were probably originated from the vertical gyro itself used as well as a rough sea condition. More minutely looking into the heading and rolling changes the roll varies with rather longer period of about 120 sec while the heading changes with a period of 80 to 100 sec(Fig.10). Such periodic noises may be generated from the Chiba University type of vertical gyro itself due to its some machnical defect. Those periodic noiseshavebeen reported from comparison of more accurate vertical gyro of the R/V Hakuho and one of the Chiba University by (Kitahara *et al.*, 1993). Noises in measurements of the ship's tilt angles would inevitably inroduce errors in calculating geomagnetic fields becuase the ship's behavior data are included in estimating the ship's induced and permanent magnetic field.

In Fig.11 the observed three components for the ship's coordinate are plotted together with the differences between the observed field and the field calculated from twelve ship's matrix constants using the "8" shaped rotation data of three different locations. Pretty large differences are found in all the component even if the differences of component to the heading are smaller than other two components. The differences of the starboard component and downward component change with a apparent period and a large value. Such a

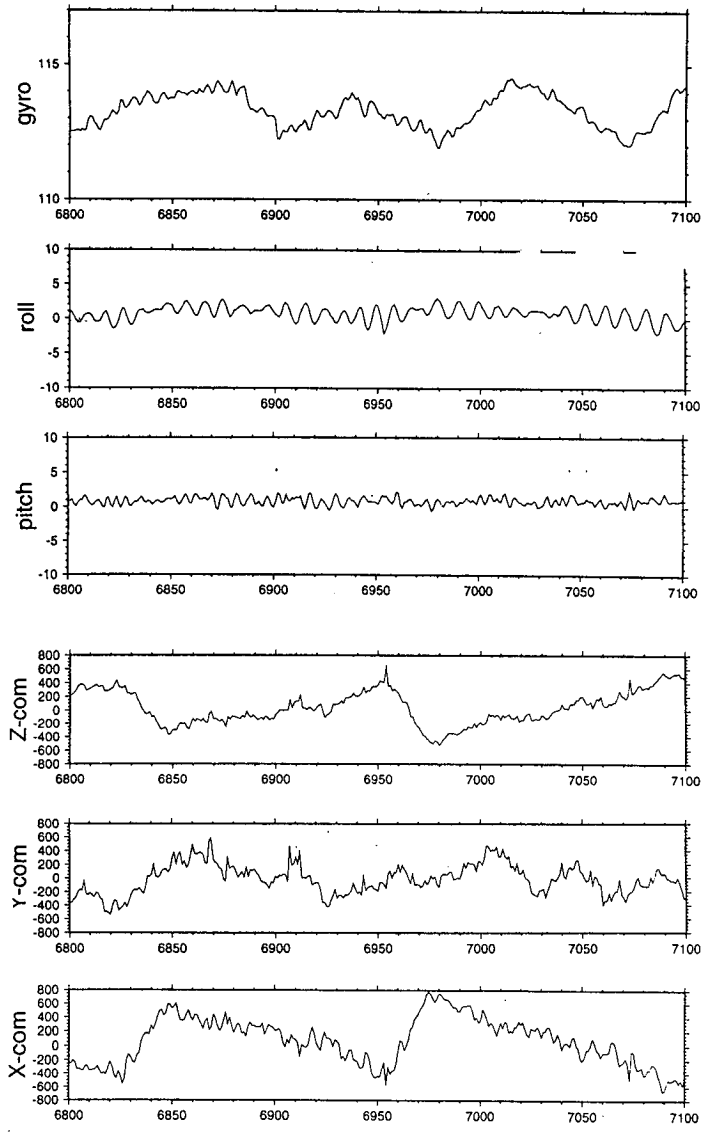

Fig.10. Erratic estimation of three component anomalies caused by gyro's noises.

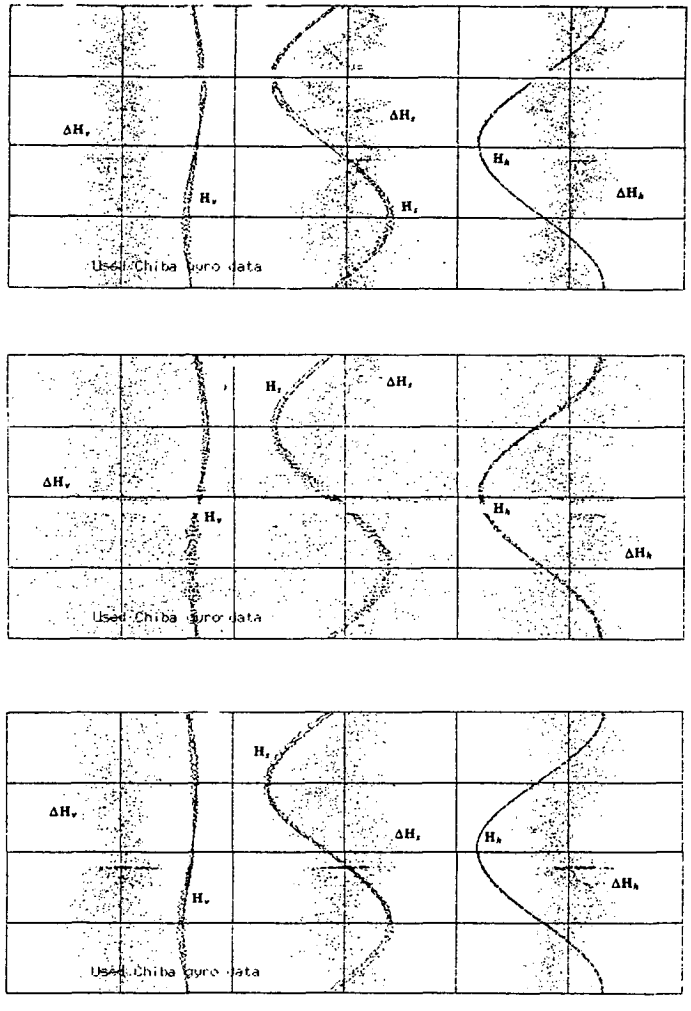

Fig.11. The variation of magnetic fields for three axes in the ship's coordinate and discrepancies between the observed field and one calculated by 12 constants at three different locations.The vertical axis indicates the heading angle from 0 to 360 degrees. The horizontal axis shows the change of magnetic fields of $\mathbf{H}_v$ (observed heading component), $\mathbf{H}_s$(observed starboard component),$\mathbf{H}_h$(observered vertical component) and $\Delta\mathbf{H}_v$, $\Delta\mathbf{H}_s$, and $\Delta\mathbf{H}_h$ are the differences between the observed field and the calculated one by 12 constants.

phenomena requires to keep us more deeply considering careful treatment of the ship's tilt data to obtain the geomagnetic field of higher precision. This preliminary processing still ignored such variation in separating the geomagnetic field from the measurement, but clearing of those noises will be followed in further processing. The effect from periodic noises of the heading, rolling and pitching could be reduced by filtering them the changes with a period longer than the specific period.

Magnetic anomalies were calculated for three component and total intensity in the earth's coordinate after the ship's magnetic, the IGRF90, and a linear trend are cleared from the observed. Fig. 6 shows three component magnetic anomaly profiles calculated and a comparison of the total intensity anomaly from three components and a proton precession anomaly. The Y component still seems to be overestimated showing periodic features and large changes in amplitude whereas X and Z components relatively keep stable. Erratic estimation in mainly the Y component is strongly related with a low quality of the gyro data. Nevertherless is the total intensity anomaly profile relatively consistent with the proton anomaly profile in general trend and amplitude.

Figs. 12,13,and 14 are plots of the three components anomalies along the tracks. The X and Z component anomalies appear to be generally normal whereas the Y component anomalies show much higher amplitude than other two components indicating that they are likely overestimated due to bad gyro data, especially, unstable rolling data. The Y component will not be taken into in geological interpretation because of its unreliablity.

Three component anomalies are generally distributed trending in the direction of SW-NE somewhat matching with a shape of the basin lengthen southwestward to northeastward. Especially the Z component and total anomaly show similar distributions with nearly same amplitude and location. The X component, however, are over the area shifted southward in its phase with reference to Z component over the area except for the west margin and the northwest of the basin southward where the anomalies are little shifted. It indicates that most of subsurface bodies are expected to be magnetized by the

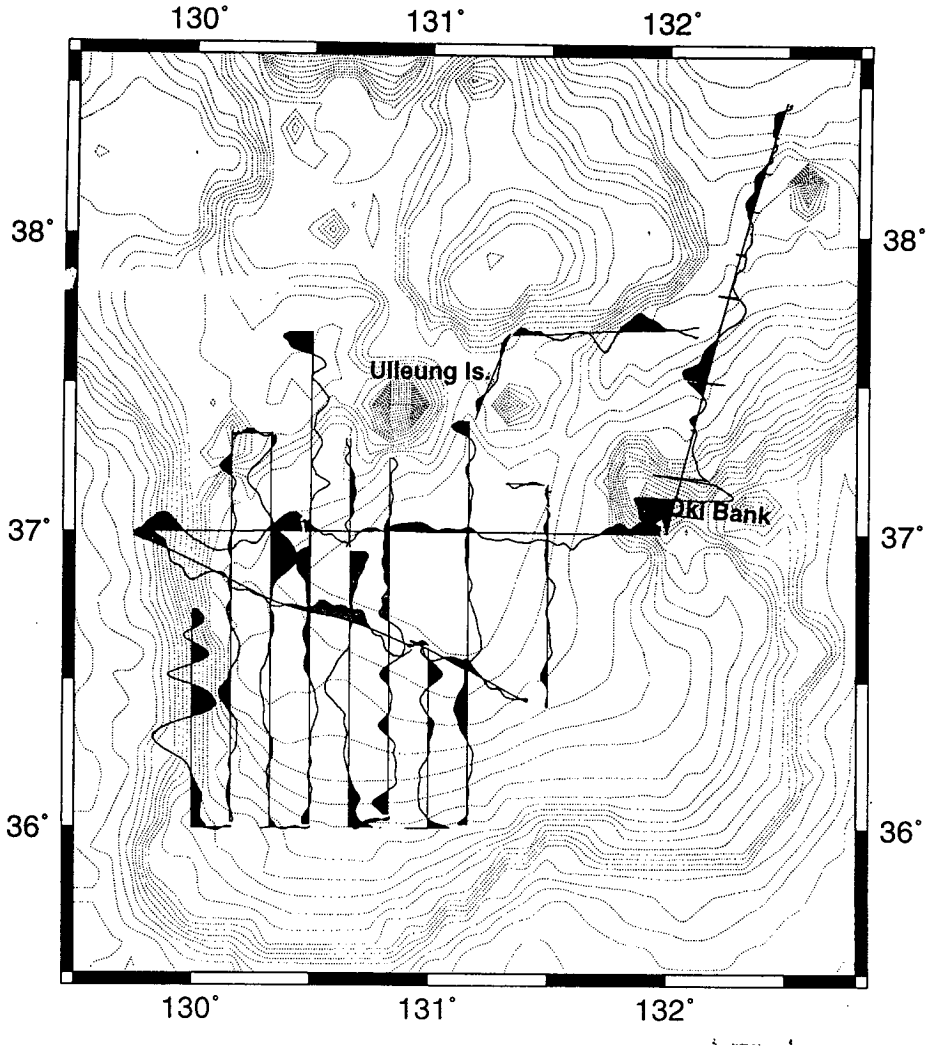

Fig.12. Geomagnetic anomaly profiles of northward component along the survey tracks. Positive anomalies are shaded.

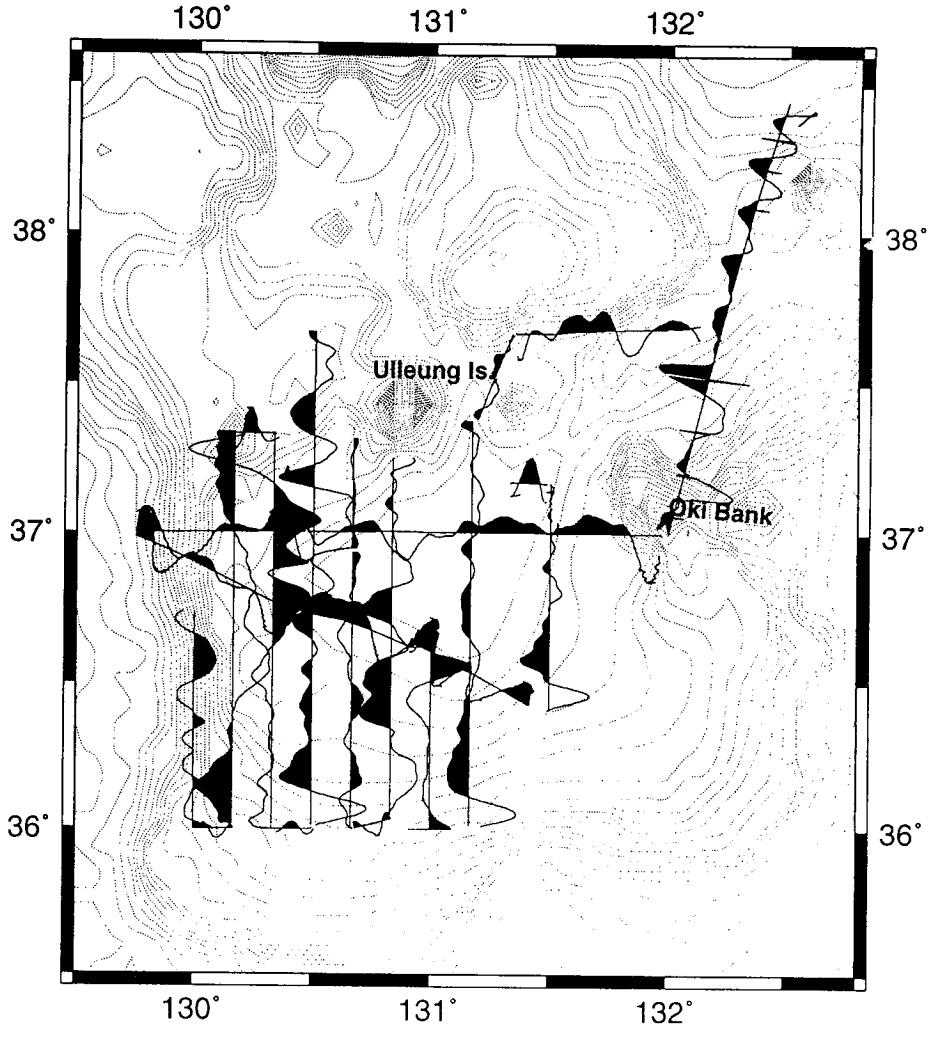

Fig.13. Geomagnetic anomaly profiles of eastward component along the survey tracks. Positive anomalies are shaded.

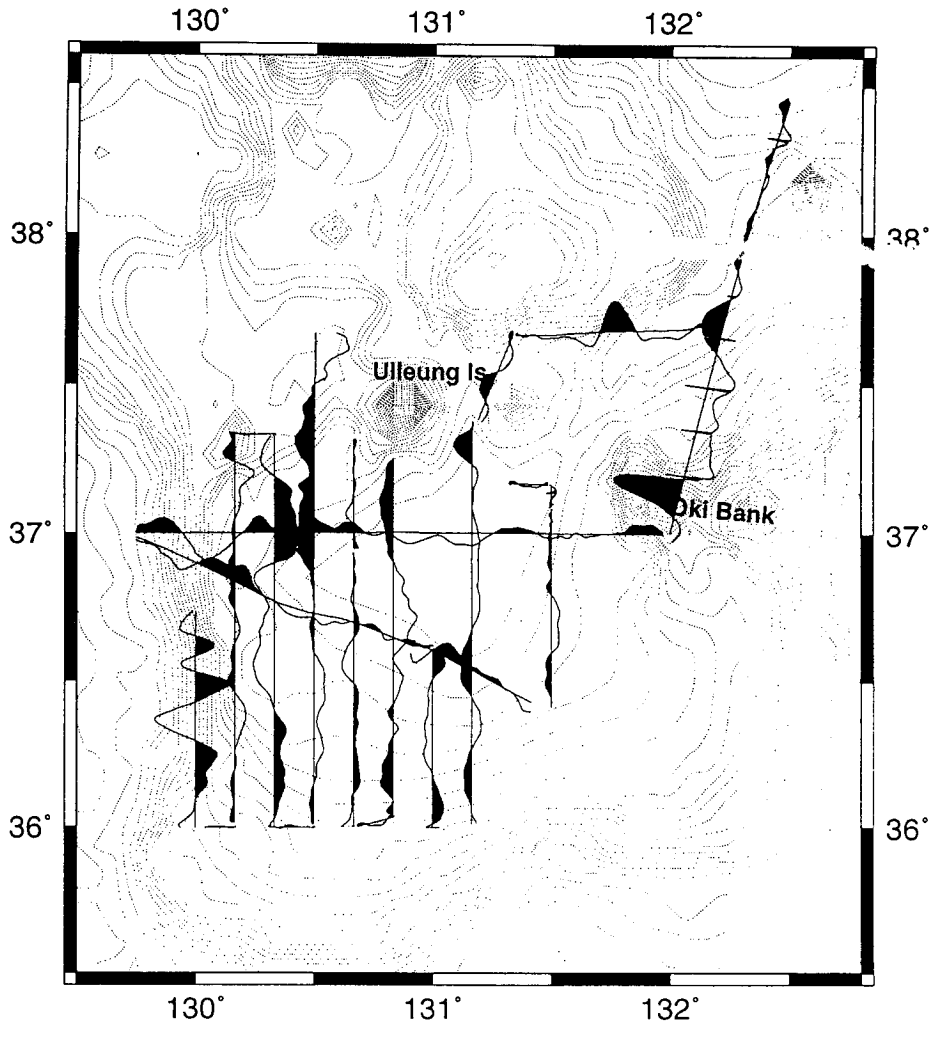

Fig.14. Geomagnetic anomaly profiles of downward component along the survey tracks.Positive anomalies are shaded.

earth's magnetic fields with a relatively steep inclination. The X and Z component anomaly as well as total anomaly(Fig.15, Fig.16) in the east of the Ulleung Island are negatively zonned trending from the SW to the NE. It reflects the existence of the shallow hot sources suggested as a result of heat flow modeling and deep seismic refraction(Suk*et al.*, 1993).

The acoustic basement in the basin center appears at depth of 5-6 secs in two way travel time below sea leve showing the characteristics similar to that of the Yamato Basin which consists of volcanic sills and flows(Chough and Lee, 1992) . In the basin center could be zonned by negative anoamly area of the Z component enclosed with positive anomaly zone of the north and south with a trend of SW to NE. Such a negative anomaly zone is possibly formed by deep basement underlain by a thick sediment. Local positive anomalies in the basin indicate that the basement would be rugged with some reliefs or intrusions.

The recent result of deep seismic refraction survey in the Ulleung Basin(Suk *et al.*, 1993) shows that the crust of the Ulleung Basin(the Tsushima Basin) has a thickness of about 13 km in the center of the basin which is twice that of the oceanic, whereas the velocity structure appears as a chacteristics of the oceanic one similar to that of the Yamato Basin. Magnetic lineations are seldom identified on maps of three component vector anomaly. The map of position and magnetic boundaries(Fig.17) also shows that there are not traced any major linear trends even though the calculation of them contains some unreliablity due to errotic estimation of Y component anomalies. Such a distribution of magnetic anomalies indicates that the basin was possibly formed by a crustal thining as a result of an extension rather than by seafloor spreading.

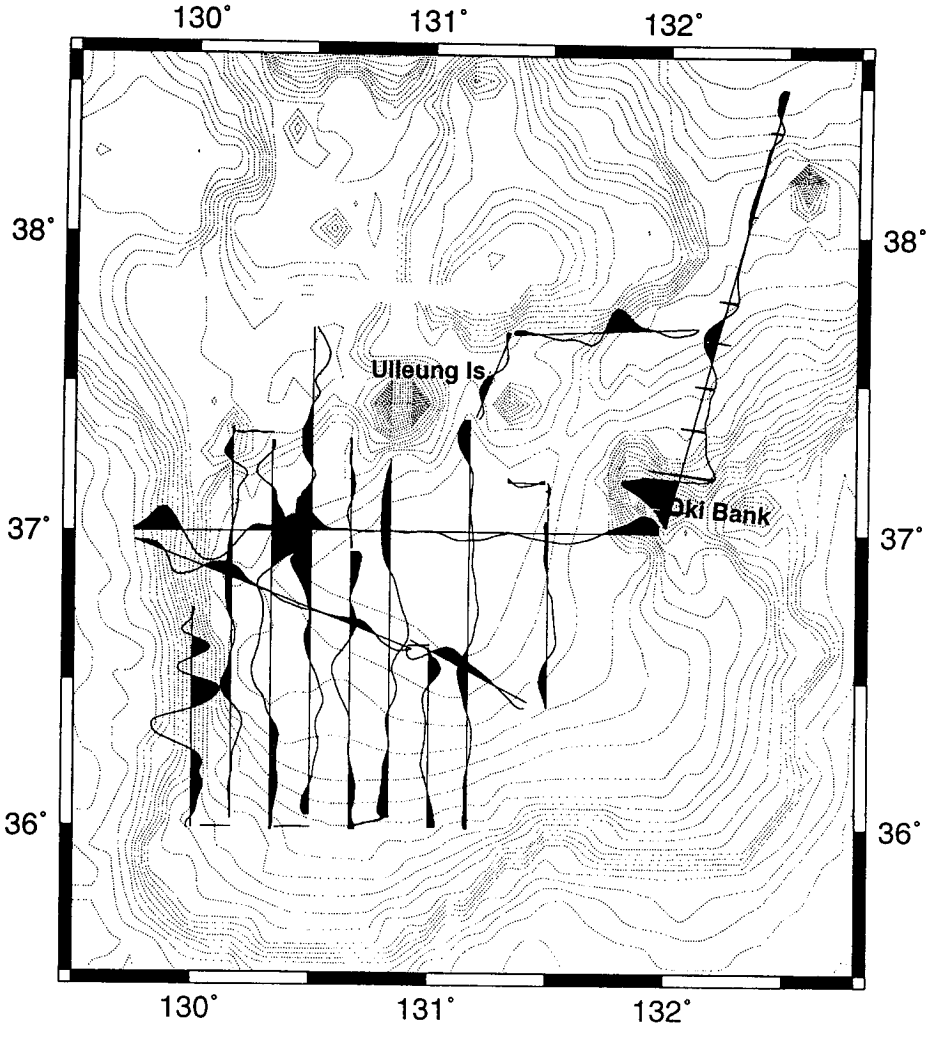

Fig.15. Total magnetic anomaly profiles from the STCM along the survey tracks. Positive anomalies are shaded.

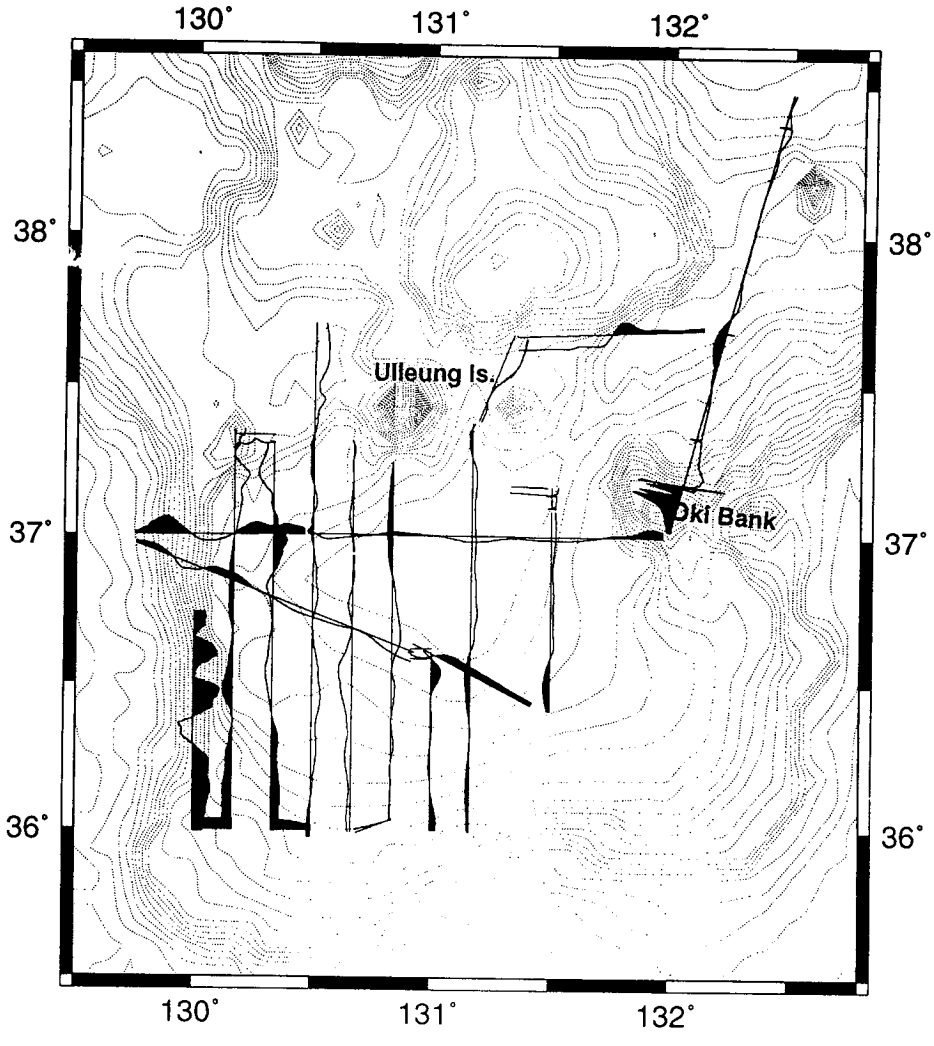

Fig.16. Total magnetic anomaly profiles from the proton precession gradiometer along the survey tracks. Positive anomalies are shaded.

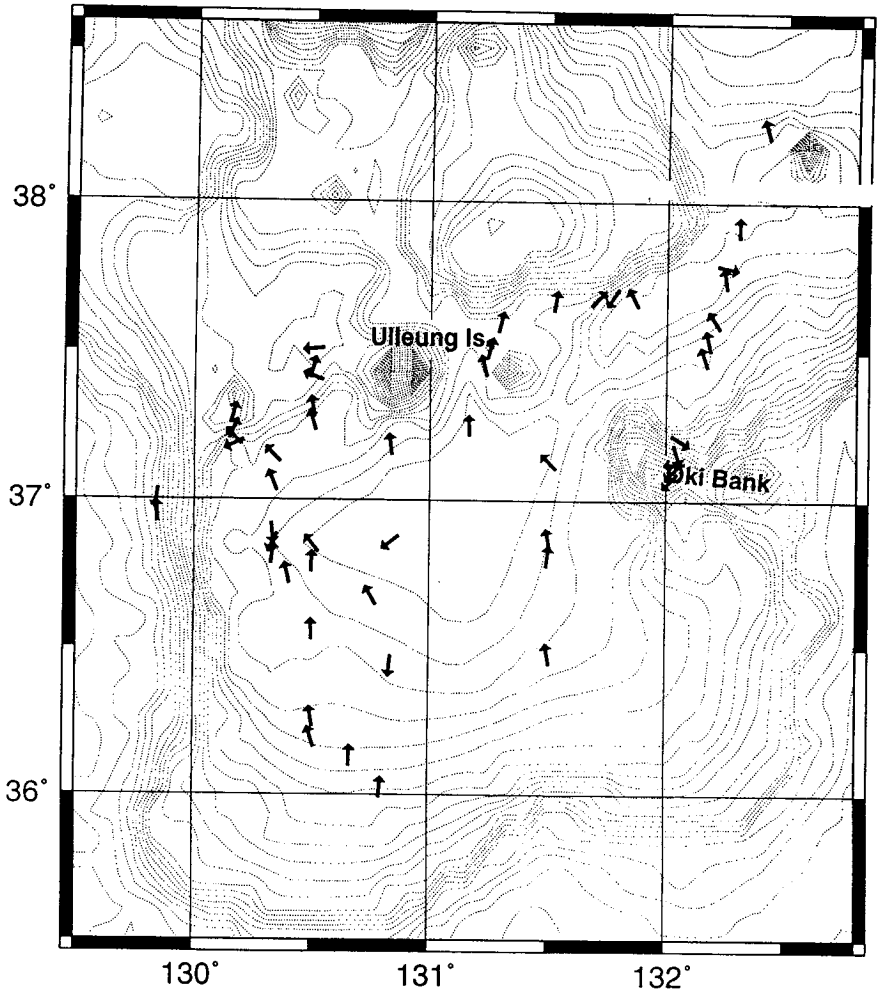

Fig.17. Magnetic boundary strike diagram. Arrow bars indicate strikes of magnetic boundary and arrow direction shows dipping of magnetic boundary.

REFERENCES

Chough,S.K. and K.E. Lee. 1992. Multi-stage volcanism in the Ulleung Back-arc Basin, East Sea(Sea of Japan). The Island Arc 1: 32-39.

Isezaki,N., J. Matsuda, H. Inokuchi and K. Yasukawa. 1981. Shipboard measurement of three components of geomagnetic field. J. Geomag. Geoelectr. 33: 329-333.

Isezaki, N. 1986. A new shipboard three component magnetometer. Geophys. 51(10): 1992-1998.

Kitahara,Y., N. Isezaki and H. Katao. 1984. Report on DELP 1984 cruises in the middle Okinawa Trough Part 3: Measurement of the three components of the geomagnetic field. Bull. Earthq. Res. Inst., Univ. Tokyo 61: 203-249.

Kitahara,A., K. Sayanagi, J. Korenaga and N. Isezaki. 1993. Preliminary report of the Hakuho Maru cruise KH 92-2, July 17-August 10, 1992. Ocean Res. Ins., Univ. of Tokyo.

Korenaga, J. 1994. The comprehensive analysis of marine magnetic vector anomalies. Summited to J. Geophys Res., Jan. 28.

Nogi,Y., N. Seama, N. Isezaki, M. Funaki and Kaminuma. 1990. Preliminary report of three components of geomagnetic field measured on board the icebreaker Shirase during JARE-30, 1988-1989. proc. NIPR Symp. Antarct. Geosci. 4: 191-200.

Press, W.H., S.A. Teukolsky, W.T. Vettering and B.P. Flannery. 1992. Numerical Recipes in C 2nd Edition. Cambridge University Press.

Seama, N., T. Ichikita and N. Isezaki. 1990. Measurement of three component component geomagnetic field by STCM. Preliminary Report of the Hakuho Maru Cruise KH-89-1, 50-57, ed. Segawa,J.,Ocean Research Institute, University of Tokyo.

Seama, N. and N. Isezaki. 1990. Seafloor magnetization in the eastern part of the Japan Basin and its tectonic implications, eds Kono, M. & Burchfiel, B. C., Tectonophysics 181: 285-297.

Seama, N., Y. Nogi and N. Isezaki. 1993. A new method for precise

determination of the position and strike of magnetic boundaries using vector data of the geomagnetic anomaly field. Geophy. J. Int. 113: 155-164.

Suh, M.C., B.C. Suk and M.K. Lee. 1993. Geological structure of the Ulleung Basin from marine gravity data. Jour.Geo.Soc.Korea 9(2): 119-127.

Suh B.C., H.J. Kim., C.H. Park, M.U. Park, G.I. Anosov. 1993. An oceanographic study in the East Sea(the Sea of Japan):Korea and Russia coorperative research. KORDI Report, 280p.